

Damping of visco-resistive Alfvén waves in solar spicules

Z Fazel and H Ebadi

Astrophysics Section, Department of Physics, University of Tabriz, Tabriz, Iran
E-mail: z_fazel@tabrizu.ac.ir

(Received 22 December 2013 , in final form 27 October 2014)

Abstract

Interaction of Alfvén waves with plasma inhomogeneity generates phase mixing which can cause the dissipation of Alfvén waves. We investigated the dissipation of standing Alfvén waves due to phase mixing at the presence of steady flow and sheared magnetic field in solar spicules. Moreover, the transition region between chromosphere and corona was considered. Our numerical simulation showed that the phase mixing and dissipation rate of Alfvén waves are enhanced relative to viscosity and resistivity gradients. Comparison of the results of our models with and without these gradients illustrated a significant difference between them. In other words, with these assumptions, Alfvén waves may transfer the photospheric energy to the corona during timescales corresponding to the observed lifetimes of spicules. It should be noted that the results of our numerical simulation were in good agreement with observational scaling law obtained by Kuridze *et al.* [1].

Keywords: solar spicules, Alfvén waves, damping, transition region.

1. Introduction

In spite of having gained knowledge and understanding about the solar atmosphere by both observations and theoretical studies, the problem of coronal heating still remains elusive. The discovery of lines of multiply ionized iron in the solar coronal spectrum [2] raised an important problem of why the temperature of the corona is 100 times larger than the temperature of the photosphere. The first idea was Alfvén waves [3] which are generated by the turbulence in the convection zone and propagate along the magnetic field lines. On each magnetic field line, Alfvén waves propagate with their local Alfvén speed. After a certain time and distance, as height increases, perturbations by Alfvén waves of neighboring magnetic field lines go out of phase and find different wavelengths, which cause large gradients in Alfvén wave front in the direction of the inhomogeneity. That is called the phase mixing which dissipates Alfvén waves [4]. This effect leads to the generation of smaller and smaller transverse spatial scales. The generation of transverse gradients in the wave leads to a strong increase in the dissipation of Alfvén wave energy due to viscosity and/or resistivity, because the dissipation is proportional to the wave number squared [5]. The energy dissipated in the wave may heat the coronal plasma [6-11]. Kudoh, considered a photospheric random motion propagating along an open magnetic flux tube in

the solar atmosphere, and performed MHD simulations for solar spicule formation and the coronal heating [12]. They have shown that Alfvén waves transport sufficient energy flux into the corona.

De Pontieu *et al.*, estimated the energy flux carried by transversal oscillations generated by spicules and indicated that the calculated energy flux is enough to heat the quiet corona and to accelerate the high-speed solar wind [13]. The phase mixing of standing Alfvén waves has been studied in the case of shear flows and fields by Ebadi *et al.* [14]. It is determined that the shear flow and field can enhance the damping of standing Alfvén waves. Smith *et al.*, have showed that the enhanced phase mixing can occur both with density gradients and sheared magnetic fields [15]. Fazel and Ebadi, have considered the effect of the transition region on the phase mixing of standing Alfvén waves in solar spicules [16]. They have concluded that phase mixing can occur in time rather than in space for these waves. Moreover, the transition region can be considered as a factor that can accelerate damping rates.

Spicules make one of the most fundamental components of the solar chromosphere. They are seen in spectral lines at the solar limb at speeds of about 20-25 km/s propagating from photosphere into the magnetized low atmosphere of the sun [17]. Their diameter and length vary from spicule to spicule having

the values from 400 km to 1500 km and from 5000 km to 9000 km, respectively. Their typical lifetime is 5-15 min. Kukhianidze *et al.*, and Zaqarashvili *et al.*, observed their transverse oscillations with the estimated period of 20-55 and 75-110 s by analyzing the height series of H α spectra in solar limb spicules observed [18,19]. Recently, Ebadi *et al.* based on Hinode/SOT observations estimated the oscillation period of spicule axis around 180 s. They concluded that the energy flux stored in spicule axis oscillations is of order of coronal energy loss in quiet Sun [20]. Okamoto *et al.*, investigated the statistical properties of Alfvénic waves in solar spicules based on SOT/Hinode observations [21]. They observed a mix of upward and downward propagating as well as standing waves. They found the occurrence rate of 20 % for standing waves. They concluded that in some spicules there are waves propagating upward and downward to form a standing wave in the middle of the spicule.

In this paper, we propose that viscosity and resistivity coefficients of the considered plasma can vary with height due to the presence of transition region between solar chromosphere and corona. The main idea is to study the effect of these inhomogeneities on dissipation of standing Alfvén waves by phase mixing. Section 2 gives the basic equations and theoretical model. In section 3, numerical results are presented and discussed, and a brief summary is followed in section 4.

2. Theoretical modeling

We consider effects of the stratification due to gravity in 2D x-z plane in the presence of steady flow and shear field. The phase mixing and the dissipation of standing Alfvén waves are studied in a region with non-uniform Alfvén velocity both along and across the spicule axis. Non-ideal MHD equations in the plasma dynamics are as follows:

$$\rho \frac{\partial \vec{V}}{\partial t} + \rho(\vec{V} \cdot \nabla) \vec{V} = -\nabla p + \rho \vec{g} + \frac{1}{\mu_0} (\nabla \times \vec{B}) \times \vec{B} + \rho \nu \nabla^2 \vec{V}, \quad (1)$$

$$\frac{\partial \vec{B}}{\partial t} = \nabla \times (V \times \vec{B}) + \eta \nabla^2 \vec{B}, \nabla \cdot \vec{B} = 0, \quad (2)$$

$$P = \frac{\rho RT}{\mu}, \quad (3)$$

where μ_0 is the vacuum permeability and μ is the mean molecular weight. $\nu(z)$, the viscosity coefficient which is defined for a fully ionized H plasma by $\rho \nu(z) = 2.2 \times 10^{-17} T_0(z)^{5/2}$ kg/ms. and $\eta(z)$ is the resistivity coefficient which is defined as a typical value in the solar chromosphere and corona by $\eta(z) = 8 \times 10^8 - 10^9 T_0(z)^{-3/2}$ m²/s [22], where the temperature profile is taken as a smoothed step function, i.e.:

$$T_0(z) = \frac{1}{2} T_c \left[1 + \frac{T_{ch}}{T_c} + \left(1 - \frac{T_{ch}}{T_c} \right) \tanh\left(\frac{z - z_t}{z_\omega}\right) \right] \quad (4)$$

where, $T_{ch} = 15 \times 10^3$ K, is the chromospheric temperature at its lower part and $T_c = 1 \times 10^6$ K is the coronal

temperature that is separated from the chromosphere by the transition region. $z_\omega = 200$ km is the width of transition region which is located at the $z_t = 2000$ km above the solar surface.

We assume that spicules are highly dynamic with speeds that are significant fractions of the Alfvén speed. Perturbations are assumed to be independent of y , i.e.:

$$\vec{V} = v_0 \hat{k} + v_y(x, y, z) \hat{j}, \quad (5)$$

$$\vec{B} = B_0 e^{-k_b z} [\cos(k_b(x-a)) \hat{i} - \sin(k_b(x-a)) \hat{k}] + b_y(x, z, t) \hat{j}, \quad (6)$$

where a is the spicule radius, and the equilibrium sheared magnetic field is two-dimensional and divergence-free [23]. Since the equilibrium magnetic field is force-free, the pressure gradient is balanced by the gravity force, which is assumed to be $\vec{g} = g \hat{k}$ via this equation:

$$-\nabla p_0(x, z) + \rho_0(x, z) \vec{g} = 0, \quad (7)$$

where the pressure in an equilibrium state and the density profile are as shown below:

$$p_0(x, z) = p_0(x) \exp\left(-\int_{z_r}^z \frac{dz'}{\Lambda(z')}\right), \quad (8)$$

$$\rho_0(x, z) = \frac{\rho_0(x) T_0}{T_0(z)} \exp\left(-\int_{z_r}^z \frac{dz'}{\Lambda(z')}\right), \quad (9)$$

where $\rho_0(x)$ is obtained from the Alfvén velocity for a phase mixed and stratified atmosphere due to gravity, which is assumed to be [24, 25]:

$$\rho_0(x) = \rho_0 \left[2 + \tanh(\alpha(x-a)) \right]^{-2}, \text{ where } \rho_0 \text{ is the plasma density at } z=5000 \text{ km, } \alpha \text{ controls the size of inhomogeneity across the magnetic field, and } \Lambda(z) = \frac{RT_0(z)}{\mu g}.$$

The linearized dimensionless MHD equations with these assumptions are:

$$\frac{\partial v_y}{\partial t} = \frac{1}{\rho_0(x, z)} \left[B_0(x, z) \frac{\partial b_y}{\partial x} + B_0(x, z) \frac{\partial b_y}{\partial z} \right] - v_0 \frac{\partial v_y}{\partial z} + \nu \nabla^2 v_y, \quad (10)$$

$$\frac{\partial b_y}{\partial t} = \left[B_0(x, z) \frac{\partial v_y}{\partial x} + B_0(x, z) \frac{\partial v_y}{\partial z} \right] - v_0 \frac{\partial b_y}{\partial z} + \eta \nabla^2 b_y, \quad (11)$$

where densities, velocities, magnetic field, time and space coordinates are normalized to ρ_0 (the plasma density at dimensionless $z=20$), V_{A0} , B_0 , τ , and a (spicule radius), respectively. Also the gravity acceleration is normalized to a^2/τ . Second terms on the left hand side of eqs. (10), (11) present the effect of steady flows. eqs. (10), (11) should be solved under following initial and boundary conditions:

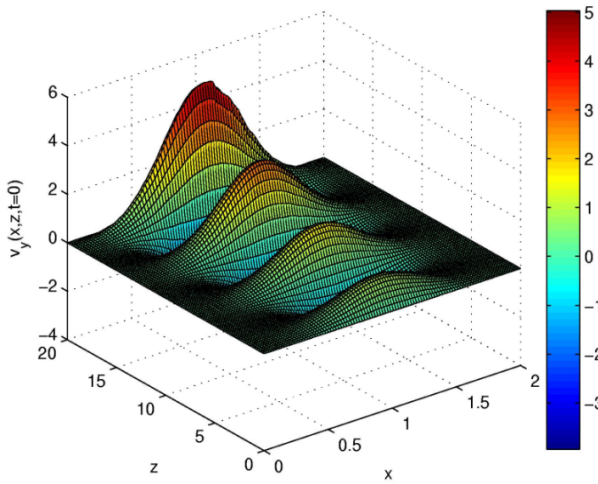


Figure 1. (color online) The initial wave packet for $d=0.3a$ is shown.

$$v_y(x, z, t = 0) = V_{A0} \exp \left[-\frac{1}{2} \left(\frac{x-1}{d} \right)^2 \right] \sin(kz) e^{z/4H} \quad (12)$$

$$b_y(x, z, t = 0) = 0,$$

where d is the width of the initial packet.

$$\begin{aligned} v_y(x=0, z, t) &= v_y(x=2, z, t) = 0, \\ b_y(x=0, z, t) &= b_y(x=2, z, t) = 0, \\ v_y(x, z=0, t) &= v_y(x, z=20, t) = 0, \\ b_y(x, z=0, t) &= b_y(x, z=20, t) = 0. \end{aligned} \quad (13)$$

Figure 1 shows the initial wave packet given by eq (12). for $d=0.3a$ (a is the spicule radius). The parameter k is chosen in a way to have the standing Alfvén wave.

3. Numerical results and discussion

To solve the coupled eqs. (10, 11) numerically, the finite difference and the Fourth-Order Runge-Kutta methods are used to take the space and time derivatives, respectively. We set the number of mesh-grid points as 256×256 . In addition, the time step is chosen as 0.0005, and the system length in the x and z dimensions (simulation box sizes) are set to be (0, 2) and (0, 20). The parameters in spicule environment are as follows: $a=250$ km (spicule radius), $d=0.3a=75$ km (the width of Gaussian packet), $L=5000$ km (Spicule length), $v_0=25$ km/s, $n_e=11.5 \times 10^{16} \text{ m}^{-3}$, $B_0=1.2 \times 10^{-3}$ Tesla, $T_0=14000$ K, $g=272 \text{ m/s}^2$, $R=8300 \text{ m}^2/\text{sK}$ (universal gas constant), $V_{A0}=75$ km/s, $\mu=0.6$, $\tau=20$ s, $\rho_0=1.9 \times 10^{-10} \text{ kg/m}^3$, $p_0=3.7 \times 10^{-2} \text{ N/m}^2$, $\mu_0=4\pi \times 10^{-7}$ Tesla m/A, $z_r=5000$ km (reference height), $z_\omega=200$ km, $z_i=2000$ km, $x_0=1000$ km, $z_0=125$ km, $\alpha=1$, $H=750$ km, $\eta=10^3 \text{ m}^2/\text{s}$, $k_b=\pi/16$, and $k=\pi/3$ (dimensionless wavenumber normalized to a).

Figures 2 and 3 illustrate the 3D plots of the perturbed velocity and magnetic field with respect to x, z for $t=10\tau$ s, $t=25\tau$ s, and $t=50\tau$ s. At the presence of the mentioned gradients and stratification due to gravity, the damping process takes place in time rather than in space. It

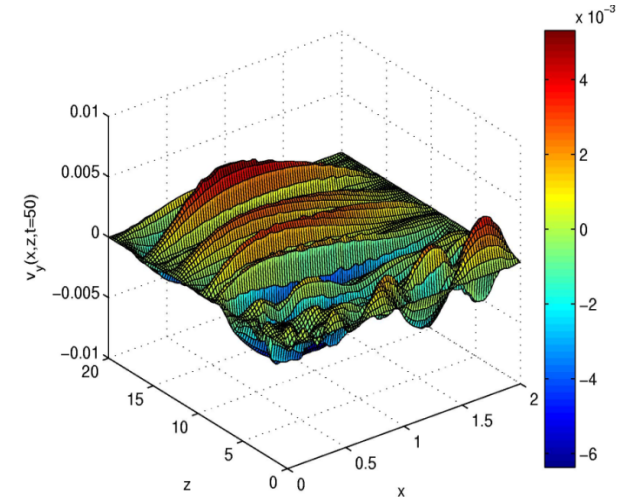
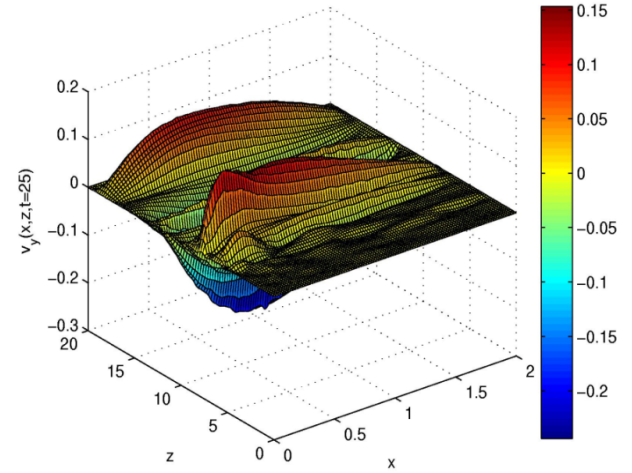
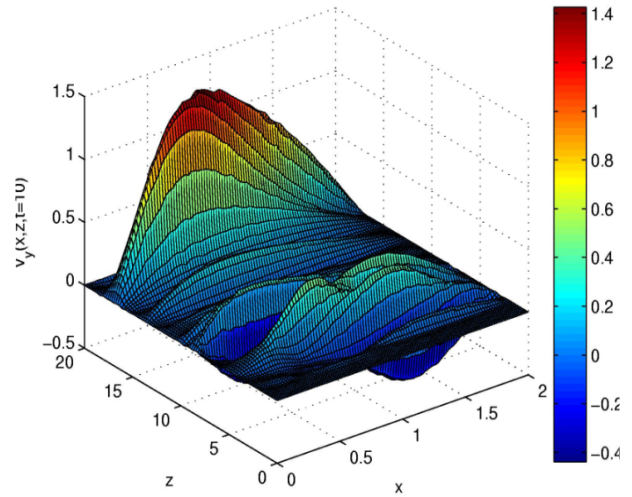


Figure 2. (color online) The 3D plots of the transversal component of the perturbed velocity with respect to x, z in $t=10\tau$ s, $t=25\tau$ s, and $t=50\tau$ s for $k_b=\pi/16$.

It should be noted that due to the initial conditions, the damping time scale for the velocity field pattern is longer than the magnetic field one.

Figure 4 shows perturbed velocity variations with respect to time in $x=250$ km, $z=875$ km; $x=250$ km, $z=2500$ km; and $x=250$ km, $z=4250$ km, respectively. In figure 5, perturbed magnetic field variations are

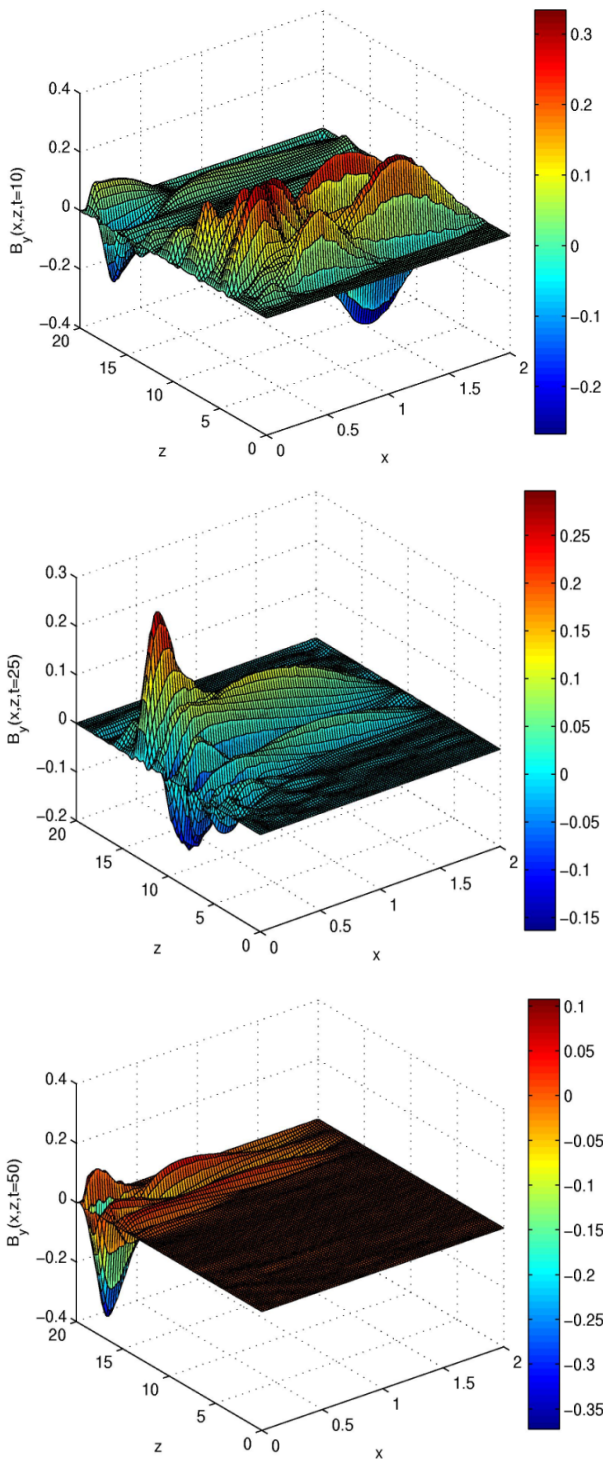


Figure 3. (color online) The same as figure 2 for the perturbed magnetic field.

presented for $x= 250$ km, $z= 875$ km; $x= 250$ km, $z= 2500$ km; and $x= 250$ km, $z= 4250$ km, respectively. In these figures, the perturbed velocity and magnetic field are normalized to V_{A0} and B_0 , respectively, and it is obvious from the plots that the damping takes place at the first stage of phase mixing. This behavior can be related to the viscosity and resistivity gradients due to

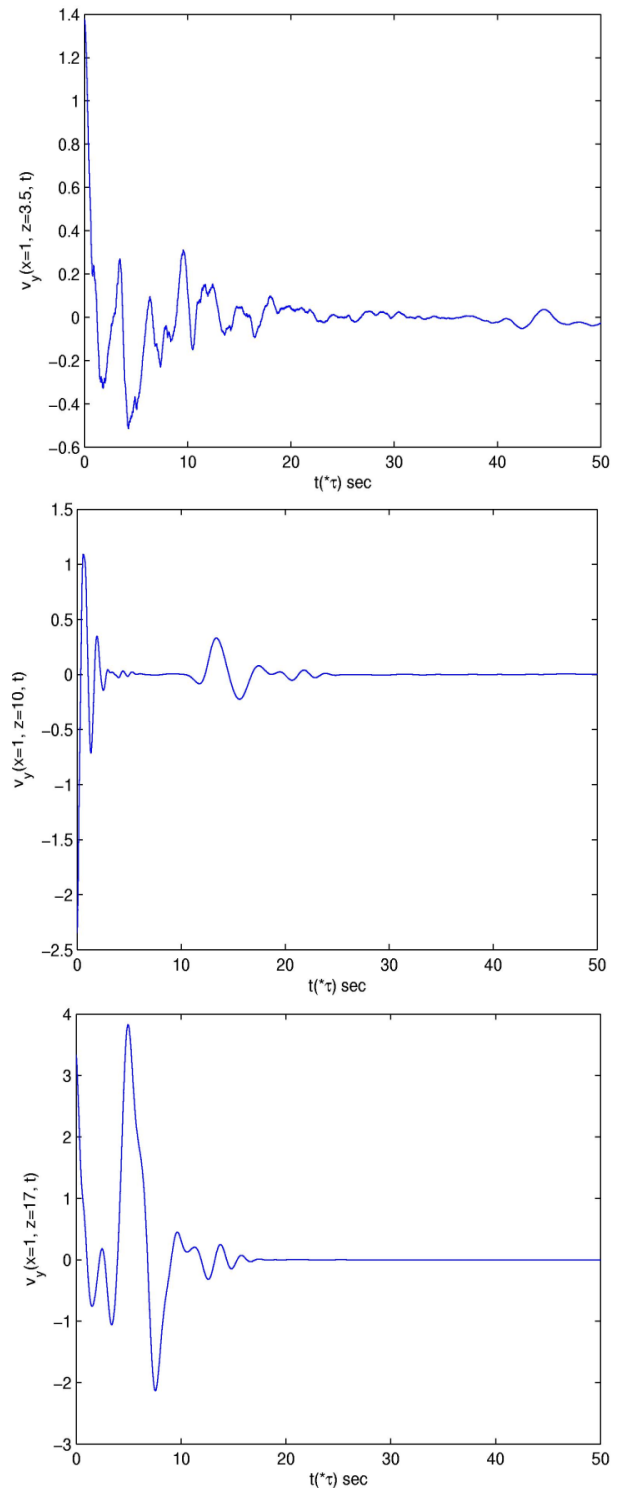


Figure 4. The perturbed velocity variations are shown with respect to time and $x= 250$ km for three values of $z= 875$ km, $z= 2500$ km, and $z= 4250$ km from top to bottom.

the presence of transition region between chromosphere and corona.

At the first height ($z= 875$ km), total amplitude of both velocity and magnetic field oscillations have values close to the initial ones. As height increases, the perturbed velocity amplitude does increase in contrast to

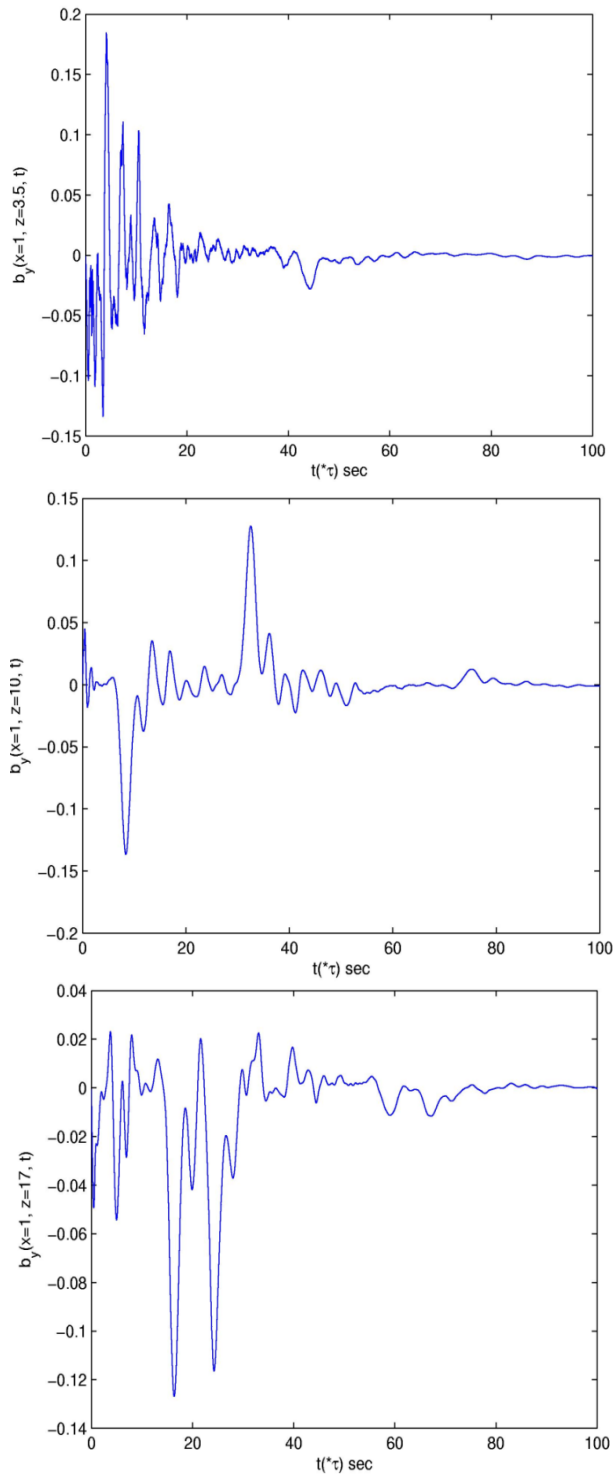


Figure 5. The perturbed magnetic field variations are shown with the same coordinates as inferred in figure 4.

the behavior of perturbed magnetic field. Nonetheless, exponentially damping behavior is obvious in both cases. This means that with an increase in height, amplitude of velocity oscillations is expanded due to significant decrease in density, which acts as inertia against oscillations. Similar results are observed by time-distance analysis of solar spicule oscillations [20]. It is worth noting that the density stratification influencing

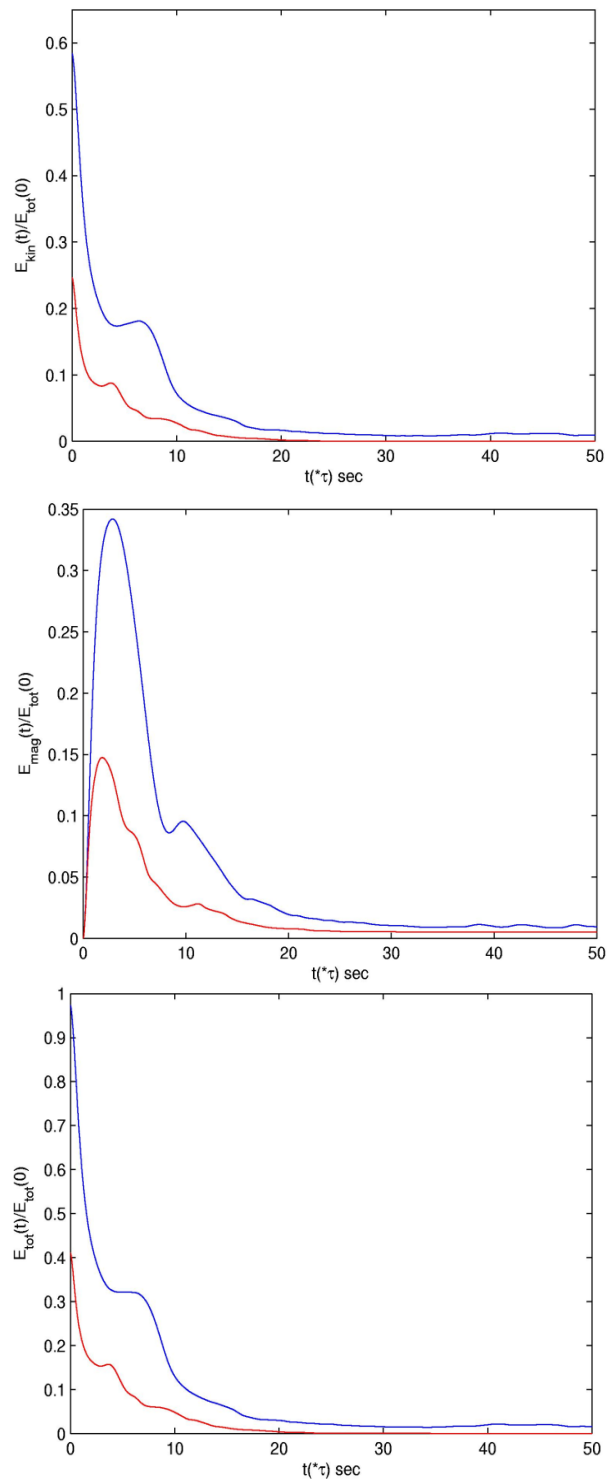


Figure 6. (color online) Time variations of the normalized kinetic, magnetic and total energies for $d= 0.3a$. Red plots show results of our model at the presence of visco-resistive gradients in Alfvén waves, the blue ones are in absence of these gradients.

the magnetic field is negligible, which is in agreement with solar optical telescope observations of solar spicules [26].

In figure 6, kinetic, magnetic and total energies normalized to the initial total energy are presented from

top to bottom, respectively. Plots with red colors show the results of our model at the presence of visco-resistive gradients in Alfvén waves. The proper plots are presented from our last model (without gradients) in blue colors. Our results show that the presence of the mentioned gradients accelerates the dissipation of Alfvén waves by phase mixing.

Since the presence of transition region leads to the variation of viscosity and resistivity coefficients, these inhomogeneities can change the rate of damping of Alfvén waves. Thus, it seems that our model will be useful to study the solar spicules. Spicules are short-lived and transient phenomena, and we conclude that the phase mixing in such circumstances can occur in time rather than in space [24]. Obtained damping times are in agreement with spicule lifetimes [17]. Estimated damping time for our presented model is about 90 s. The proper damping time determined from the scaling law presented by Kuridze *et al.*, 2012 [1] ($\tau_d = 8.34 T^{3/4}$), is 80 s. So, our numerical results are confirmed by the mentioned observational scaling law.

4. Conclusion

Study of standing Alfvén waves in solar spicules may present an efficient heating mechanism in the solar chromosphere and lower corona. In this paper, we

consider spicules with steady flow and sheared magnetic field. The non-ideal behavior of standing Alfvén waves and their phase mixing have been studied in such plasma that has inhomogeneity represented by the gradients in viscosity and resistivity coefficients. These gradients are due to the presence of transition region between chromosphere and corona. Our simulations show that phase mixing can occur in time rather than in space for standing Alfvén waves. The perturbed velocity amplitude increases as height is increased. In contrast, the perturbed magnetic field amplitude decreases with height. Both perturbed velocity and magnetic field amplitudes decrease efficiently with time. In the previous work, we showed that the transition region could be considered as a factor to accelerate damping rates of Alfvén waves in solar spicules. Now our numerical simulations show that these damping rates are enhanced relative to viscosity and resistivity gradients. A comparison of the results of our models with and without these gradients in figure 6 illustrates a significant difference between them. In both cases, we observe that energies decrease with time exponentially, but faster than the preceding work. Thus, knowing that spicules are short lived structures, the fast dissipation mechanism will be needed to deliver their energy to the corona.

References

1. D Kuridze, R J Morton, R Erdelyi, G D Dorrian, M Mathioudakis, D B Jess, and F P Keenan, *Astrophys. J.* **750** (2012) 5.
2. B Edlen, *Z. Astrophysik* **22** (1943) 30.
3. H Alfvén, *Science* **107** (1942) 211.
4. J Heyvaerts and E R Priest, *Astron. Astrophys.* **117** (1983) 220.
5. G J J Botha, T D Arber, V M Nakariakov, and F P Keenan, *Astron. Astrophys.* **363** (2000) 1189.
6. H Alfvén, *Monthly Notices of the Royal Astronomical Society* **107** (1947) 211.
7. J V Hollweg, *Astrophys. J.* **181** (1973) 547.
8. J V Hollweg, *J. Geophys. Res.* **91** (1986) 4111.
9. J F McKenzie, M Banaszekiewicz and W I Axford, *Astron. Astrophys.* **303** (1995) 45.
10. H Safari, S Taran and N Farhang, *Iranian Journal of Physics Research* **14**, 1 (2014) 65.
11. S. Nasiri and L. Yousefi, *Iranian Journal of Physics Research* **5**, 3 (2005) 145.
12. T Kudoh and K Shibata, *Astrophys. J.* **514** (1999) 493.
13. B De Pontieu *et al.*, *Science* **318** (2007) 1574.
14. H Ebadi and M Hosseinpour, *Astrophys. Space Sci.* **343** (2013) 11.
15. P D Smith, D Tsiklauri, and M S Ruderman, *Astron. Astrophys.* **475** (2007) 1111.
16. Z Fazel and H Ebadi, *Astrophys. Space Sci.* **346** (2013) 319.
17. T V Zaqarashvili and R Erdelyi, *Space Sci. Rev.* **149** (2009) 335.
18. V Kukhianidze, T V Zaqarashvili, and E Khutsishvili, *Astron. Astrophys.* **449**, (2006) 35.
19. T V Zaqarashvili, E Khutsishvili, V Kukhianidze, and G Ramishvili, *Astron. Astrophys.* **474** (2007) 627
20. H Ebadi, T V Zaqarashvili, and I Zhelyazkov, *Astrophys. Space Sci.* **337** (2012) 33.
21. T J Okamoto and B De Pontieu, *Astrophys. Letters* **736** (2011) L24, 6.
22. E R Priest, “*Solar magnetohydrodynamic*”, Reidel, Dordrecht (1982).
23. L Del Zanna, E Schaekens, and M Velli, *Astron. Astrophys.* **431** (2005) 1095.
24. I De Moortel, A W Hood, and T D Arber, *Astron. Astrophys.* **346** (1999) 641.
25. K Karami and Z Ebrahimi, *Publ. Astron. Soc. Aust.* **26** (2009) 448.
26. G Verth, M Goossens, and J S He, *Astrophys. J. Lett.* **733** (2011) 15.